

Whispering-gallery-modelike-enhanced emission from ZnO nanodisk

Chinkyoo Kim

*Department of Physics and Research Institute of Basic Sciences, Kyunghee University,
1 Hoegi-dong Dongdaemoon-gu, Seoul 130-701, Korea*

Yong-Jin Kim,^{a)} Eue-Soon Jang, and Gyu-Chul Yi^{a),b)}

*National CRI Center for Semiconductor Nanorods, and Department of Materials Science and Engineering,
Pohang University of Science and Technology (POSTECH), Pohang 790-784, Korea*

Hyun Ha Kim

*Materials Characterization Group, LG Electronics Institute of Technology, 16 Woomyeon-Dong, Seocho-Gu,
Seoul 137-724, Korea*

(Received 8 August 2005; accepted 3 January 2006; published online 27 February 2006)

Hexagonal nanodisks of ZnO were fabricated by a solution process using ZnO nanoparticles and their cathodoluminescence characteristics were investigated. Monochromatic cathodoluminescence images showed that luminescence was spatially localized near the boundary of the nanodisk and spectral analysis in conjunction with the intensity profile consistently ascribed the spatial localization of luminescence to whispering-gallery-modelike-enhanced emission. © 2006 American Institute of Physics. [DOI: 10.1063/1.2174122]

With the successful demonstration of various nanostructures and increasing demand for integrable optoelectronic components with existing silicon technology, small-scale dielectric resonators applicable to photonic nanodevices with low-thresholds have gained importance because they can be used as low-power-consumption light sources in integrated circuits. Reducing the size of photonic devices, however, results in decrease of luminescence intensity in such a way that careful design of intensity enhancement mechanism should be introduced. For this reason, the whispering-gallery mode, which has been particularly utilized in applications to optical communication, has attracted much attention because it is a very efficient mechanism of luminescence enhancement even in small-scale resonators.¹⁻⁴ Since a top-down approach, such as lithography, has been among the best technological methods to fabricate tailored nanostructures appropriate for specific research or application purposes, much effort has been made in order to fabricate nanoresonators via lithography to achieve low-threshold photonic nanodevices. There are, however, a few important generic problems in top-down fabrication of nanoresonators. There is unavoidable damage to films associated with lithographic etching process. An unwanted strain effect is also involved due to the limited choice of substrates to accommodate lattice misfit. In contrast, photonic nanodevices with bottom-up-based nanoscale resonant cavity employing whispering-gallery modes (WGMs) are very promising integrable components with high luminescence efficiency. More than that, a bottom-up approach typically does not depend on the choice of substrates, which is a major advantage in integration with current silicon technology.

Due to direct and wide-band-gap characteristics with a large binding exciton energy, ZnO has drawn much attention for potential application to short-wavelength optoelectronic devices. In addition to single-crystalline ZnO thin films, ZnO

nanowires and nanorods with perfect crystallinity were recently fabricated, and newly developed ZnO-based nanostructures demonstrated the possibility for nanoscale optoelectronic devices.⁵⁻⁷ In contrast with one-dimensional nanostructures, such as nanorods, hexagonal nanodisk resonators employing WGMs have a smaller effective volume of gain medium, so that it is easier to fabricate compact photonic nanodevices. In addition, nanodisks are more confined to the surface of substrate and mechanical stability of nanodisks for postgrowth process is superior to that of nanorods. Here, we report the first observation of WGM-like-enhanced emission from ZnO nanodisks grown on Si substrates. ZnO hexagonal nanodisks were fabricated by a solution process using ZnO nanoparticles as a seed material. Monochromatic cathodoluminescence images showed that luminescence was spatially localized near the boundary of the nanodisk, and spectral analysis in conjunction with intensity profile consistently ascribed the spatial localization of luminescence to WGM-like-enhanced emission.

Among a few methods to grow ZnO nanodisks,^{8,9} we used a soft solution process to fabricate ZnO nanodisks using ZnO nanoparticles as seeds or buffer layers for the growth. ZnO nanoparticles were prepared through a previously reported method.¹⁰ Si (100) wafer (1 cm × 1 cm) was used as a substrate for ZnO nanodisk fabrication. Si wafers were cleaned with acetone, methanol, and isopropanol by ultrasonication and etched by HF solution for 1 min. 0.1 M alcoholic ZnO nanoparticles were dipcoated or spincoated on the substrate. The nutrient solution for the ZnO nanodisk growth was prepared from an aqueous solution of 0.5 M zinc acetate, 0.2 M NaOH, and 0.17 mM sodium citrate in a 100 mL Teflon-lined autoclave as reported by Vayssieres *et al.*^{11,12} The autoclave was maintained at 95 °C for 12 h in a laboratory oven and then cooled to room temperature naturally. The product on the substrate was washed with deionized H₂O several times to remove any residual salts. The diameter and thickness of ZnO nanodisks depend on the growth conditions, ranging from 1 to 5 μm and from 50 to 200 nm, respectively. The morphology and size of ZnO

^{a)} Also at: School of Environmental Sciences and Engineering, Pohang University of Science and Technology (POSTECH), Pohang, 790-784, Korea.

^{b)} Author to whom correspondence should be addressed; electronic mail: gcyi@postech.ac.kr

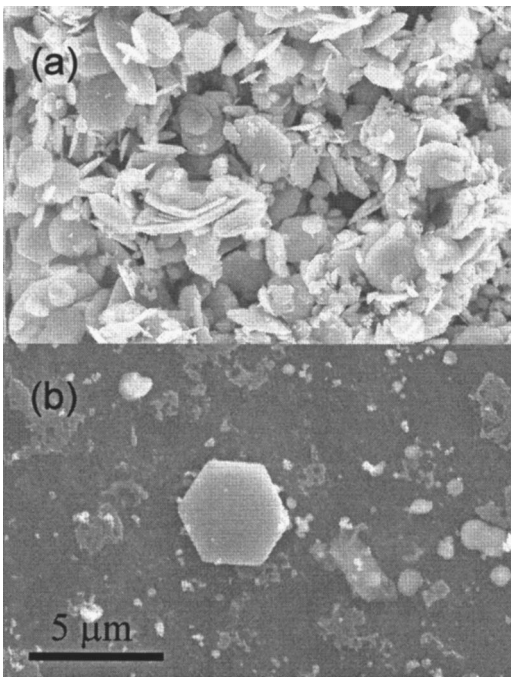


FIG. 1. (a) SEM images of ZnO hexagonal nanodisks. Densely grown nanodisks with different sizes and random orientations. (b) A vertically grown isolated nanodisk.

nanodisks were observed by field-emission scanning electron microscopy (SEM), (Philips XL30S). Cathodoluminescence measurements were carried out at room temperature with an acceleration voltage of 20 kV.

With our methods, ZnO nanodisks were easily obtained on a Si substrate, but the number density of the nanodisks varied significantly across the substrate surface as shown in Fig. 1. In the densely grown area, the ZnO nanodisks have quite random orientations [Fig. 1(a)] but, in some part, isolated ZnO nanodisks were vertically grown [Fig. 1(b)]. In order to investigate the cathodoluminescence characteristics, we chose the area in which the nanodisks are not densely distributed.

Figure 2(a) shows cathodoluminescence spectra from the vertically grown isolated hexagonal nanodisk. The main peak

is at 378 nm and there is no yellow luminescence related to deep levels.¹³ The emissions due to deep levels associated with defects in ZnO is often observed in other ZnO nanostructures,¹⁴ but our ZnO nanodisks showed strong band-edge emissions with no deep level emissions affiliated with defects, implying that our ZnO nanodisks have good crystal quality and are more appropriate for photonic nanodevices.

Shown in Fig. 2(b) is monochromatic cathodoluminescence image (at 378 nm) of a vertically oriented ZnO hexagonal nanodisk. The luminescence intensity is not uniformly distributed across the nanodisk, but it is locally concentrated near the hexagonal boundary. This type of spatial localization of intensity is typically observed in whispering-gallery modes in dielectric resonant cavities. Inside the resonant cavity, electromagnetic waves circulate with negligible loss due to multiple total internal reflection at the resonator's boundary. In particular, Wiersig¹⁵ carried out a numerical analysis of long-lived modes in hexagonal dielectric resonant cavity and showed that the intensity is concentrated near the boundary of the hexagonal resonator. Thus, we can conclude that the strong localization of intensity near the boundary is attributed to the WGM-like-enhanced emission because the luminescence distribution across the nanodisk would be uniform without WGM-like luminescence enhancement. The spatial distribution of intensity across the nanodisk is shown in Fig. 2(c), and since the stronger intensity near the boundary is due to WGM-like-enhanced emission, the darkened area under the intensity profile can be attributed to the contribution from the WGM-like-enhanced luminescence. The darkened area is about one-quarter of the total area under the intensity profile curve, so that the percentage of WGM-like-enhanced luminescence among the total luminescence is approximately 25%, which is much larger than WGM contribution observed in ZnO nanoneedles.¹⁴

To check consistency, we have made a spectral analysis to estimate the contribution of the WGM-like-enhanced luminescence. For this purpose, we have calculated the resonant wavelengths in the following way. If the total phase shift along the path during one complete turn is an integer multiple of 2π , then the standing wave is generated due to

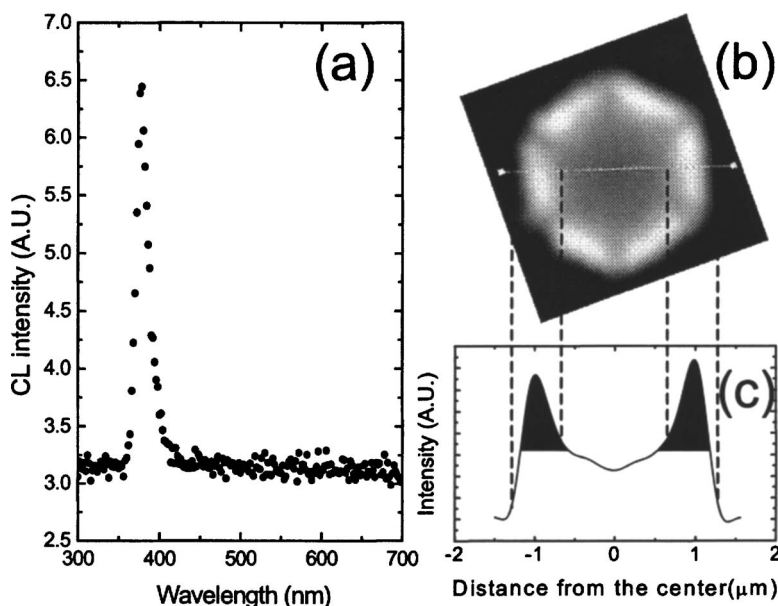


FIG. 2. (a) Cathodoluminescence spectra of a ZnO nanodisk measured at room temperature. The main peak is at 378 nm and there is no yellow emission related to deep levels. (b) Monochromatic cathodoluminescence image (at 378 nm) of a vertically oriented ZnO hexagonal nanodisk. The side length of the ZnO hexagonal nanodisk is approximately $1.6 \mu\text{m}$. (c) The intensity profile across the nanodisk. The darkened area indicates the luminescence contribution from the WGM-like-enhanced emission. Note that the darkened area is one-quarter of the total area under the intensity profile, which indicates that the contribution from the WGM-like luminescence to the total intensity is approximately 25%.

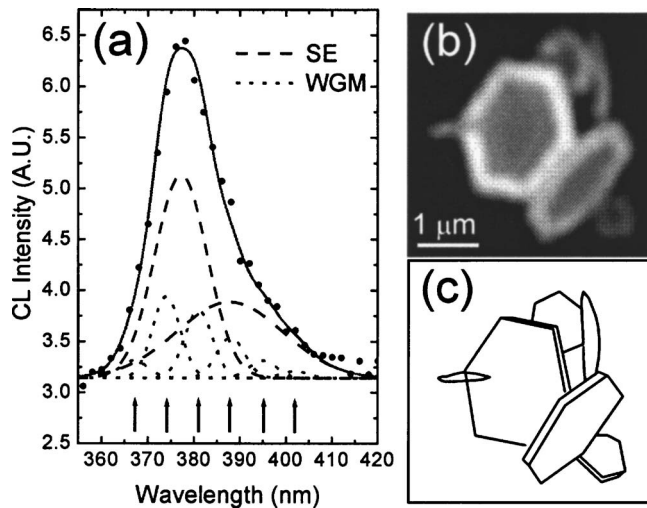


FIG. 3. (a) Blowup spectra from Fig. 2(a). Arrows mark the calculated wavelengths in WGMs. The contribution from WGM-like-enhanced luminescence were approximated with six Gaussians. Note that the total intensity was assumed to consist of two parts; spontaneous emission (two broad Gaussians) and the WGM-like-enhanced emission (relatively narrow six Gaussians). In particular, the contribution from each part is approximately 75% and 25% at 378 nm, respectively. This ratio is consistent with that obtained from the intensity profile shown in Fig. 2(c). (b) Monochromatic cathodoluminescence image (at 382 nm) of ZnO nanodisks with different orientations. Note that the tilted ZnO nanodisk also shows the spatial localization of luminescence near the boundary. (c) Schematic drawing of the nanodisks shown in (b).

constructive interference over multiple circulations. For the hexagonal resonant cavities, the constructive interference condition is given by

$$nR = \frac{\lambda}{3\sqrt{3}} \left[N + \frac{6}{\pi} \arctan(\beta\sqrt{3n^2 - 4}) \right], \quad (1)$$

where n is the index of refraction, R is the hexagonal resonant cavity side length, λ is the wavelength of light, N is the resonance interference order, β is n^{-1} (n) for transverse magnetic (TM) [transverse electric (TE)] polarization.¹⁴ The index of refraction of ZnO at 378 nm is known to be 2.5, and the calculated wavelengths in resonance can be obtained by plugging in the appropriate numbers. In Fig. 3(a), which is a blowup spectra of Fig. 2(a), the calculated wavelengths of WGM are marked by arrows. We approximated the contribution from WGM-like-enhanced luminescence with Gaussian functions centered at each resonant wavelength, but the Gaussian widths were set to be broader than those of typical lasing peaks for two reasons; first, it is below the lasing threshold, and second, the resonant wavelengths for TE and TM modes are so close that they overlap with each other resulting in broad Gaussians. The latter is because N is such a large number that the difference in β , depending on polarization, does not produce any major changes in the resonant wavelengths. It must be also noted that nanodisks do not exclude TE modes as in nanoneedles in which only TM modes were observed.^{14,16} We have fitted our data with six fixed-centered Gaussians (for the WGM-like enhanced emission) and two Gaussians (for spontaneous emission). The fitting parameters of six Gaussians for WGM-like modes were not allowed to vary freely; the peak positions were fixed and their relative intensities were constrained in accordance with the overall peak shape. As shown in Fig. 3, eight Gaussians

reproduced the luminescence intensity spectra reasonably well. With these parameters constrained, the estimated portion of the WGM-like-enhanced emission in the total intensity at 378 nm is approximately $25 \pm 10\%$, which is in good agreement with the result obtained from the spatial distribution of luminescence intensity, which confirms that the localized luminescence near hexagonal boundary is due to the WGM-like-enhanced luminescence.

It could be also argued that the nonuniform luminescence across the nanodisk may be due to extended defects, such as dislocations, through the center of the nanodisk. However, our ZnO nanodisk growth method was performed in such a way that the dislocations are not likely to be introduced because the atoms in nanodisks do not strongly bond with the substrate atoms with no need to relieve strain. In particular, as shown in Fig. 3(c), the fact that the tilted grown ZnO nanodisk, which does not experience strain at all due to lattice mismatch, also shows that the strong localization near the hexagonal boundary is strong evidence that the effect is not due to extended defects of nonrecombination centers.

For the first time, we have demonstrated the WGM-like-enhanced emission from ZnO hexagonal nanodisks. This result implies that ZnO nanodisks have potential low-threshold nanophotonics applications, but the potential application of WGM-based photonic nanodevices is not limited to ZnO. This can be extended to various materials, with which nanodisks can be fabricated. It is of great importance in nanophotonics to pursue further investigation of resonant characteristics of different materials with various nanostructures.

The work at Kyunghee University was supported by a grant (No. 05K1501-02520) from the ‘‘Center for Nanostructured Materials Technology’’ under ‘‘21st Century Frontier R&D Programs’’ of the Ministry of Science and Technology, Korea. The work at POSTECH was supported by the National Creative Research Initiative Project of the Ministry of Science and Technology.

¹S. I. Shopova, G. Farca, A. T. Rosenberger, W. M. S. Wickramanayake, and N. A. Kotov, *Appl. Phys. Lett.* **85**, 6101 (2004).

²H.-Y. Ryu, S.-H. Kim, H.-G. Park, J.-K. Hwang, Y.-H. Lee, and J.-S. Kim, *Appl. Phys. Lett.* **80**, 3883 (2002).

³V. N. Astratov, J. P. Franchak, and S. P. Ashili, *Appl. Phys. Lett.* **85**, 5508 (2004).

⁴A. Serpenguzel, T. Bilici, S. Isci, and A. Kurt, *Proc. SPIE* **5357**, 153 (2004).

⁵J. C. Johnson, H. Yan, R. D. Schaller, L. H. Harber, R. J. Saykally, and P. Yang, *J. Phys. Chem.* **105**, 11387 (2001).

⁶W. I. Park, G.-C. Yi, M. Kim, and S. J. Pennycook, *Adv. Mater. (Weinheim, Ger.)* **15**, 526 (2003).

⁷W. I. Park, and G.-C. Yi, *Adv. Mater. (Weinheim, Ger.)* **16**, 87 (2004).

⁸C. X. Xu, X. W. Sun, and Z. L. Dong, *Appl. Phys. Lett.* **85**, 3878 (2004).

⁹Z. Tian, J. A. Voigt, J. Liu, B. McKenzie, M. J. Mcdermott, M. A. Rodriguez, H. Konishi, and H. Xu, *Nat. Mater.* **2**, 821 (2003).

¹⁰L. Spanhel and M. A. Anderson, *J. Am. Chem. Soc.* **113**, 2826 (1991).

¹¹L. Vayssieres, *Adv. Mater. (Weinheim, Ger.)* **15**, 464 (2003).

¹²L. Vayssieres, K. Keis, S.-E. Lindquist, and A. Hagfeldt, *J. Phys. Chem. B* **105**, 3350 (2001).

¹³W. I. Park, Y. H. Jun, S. W. Jung, and G.-C. Yi, *Appl. Phys. Lett.* **82**, 964 (2003).

¹⁴T. Nobis, E. M. Kaidashev, A. Rahm, M. Lorenz, and M. Grundmann, *Phys. Rev. Lett.* **93**, 103903 (2004).

¹⁵J. Wiersig, *Phys. Rev. A* **67**, 023807 (2003).

¹⁶X. Liu, W. Fang, Y. Huang, X. H. Wu, S. T. Ho, H. Cao, and R. P. H. Chang, *Appl. Phys. Lett.* **84**, 2488 (2004).